JACS
JOURNAL OF THE AMERICAN CHEMICAL SOCIETY
Article
pubs.acs.org/JACS

A Transition from Localized to Strongly Correlated Electron Behavior and Mixed Valence Driven by Physical or Chemical Pressure in ACo_2As_2 (A = Eu and Ca)

Xiaoyan Tan,[†] Gilberto Fabbris,[‡,§] Daniel Haskel,[‡] Alexander A. Yaroslavtsev,[∥,⊥] Huibo Cao,[#] Corey M. Thompson,[†] Kirill Kovnir,[†] Alexey P. Menushenkov,[∥] Roman V. Chernikov,[▽] V. Ovidiu Garlea,[#] and Michael Shatruk*[,†]

[†]Department of Chemistry and Biochemistry, Florida State University, Tallahassee, Florida 32306, United States
[‡]Advanced Photon Source, Argonne National Laboratory, Argonne, Illinois 60439, United States
[§]Department of Physics, Washington University, St. Louis, Missouri 63130, United States
[∥]National Research Nuclear University MEPhI (Moscow Engineering Physics Institute), 115409, Moscow, Russia
[⊥]European XFEL GmbH, 22761 Hamburg, Germany
[#]Quantum Condensed Matter Division, Oak Ridge National Laboratory, Oak Ridge, Tennessee 37831, United States
[▽]DESY Photon Science, 22603 Hamburg, Germany

Supporting Information

ABSTRACT: We demonstrate that the action of physical pressure, chemical compression, or aliovalent substitution in ACo_2As_2 (A = Eu and Ca) has a general consequence of causing these antiferromagnetic materials to become ferromagnets. In all cases, the mixed valence triggered at the electropositive A site results in the increase of the Co 3d density of states at the Fermi level. Remarkably, the dramatic alteration of magnetic behavior results from the very minor (<0.15 electron) change in the population of the 3d orbitals. The mixed valence state of Eu observed in the high-pressure (HP) form of $EuCo_2As_2$ exhibits a remarkable stability, achieving the average oxidation state of +2.25 at 12.6 GPa. In the case of $CaCo_2As_2$, substituting even 10% of Eu or La into the Ca site causes ferromagnetic ordering of Co moments. Similar to HP-$EuCo_2As_2$, the itinerant 3d ferromagnetism emerges from electronic doping into the Co layer because of chemical compression of Eu sites in $Ca_{0.9}Eu_{0.1}Co_{1.91}As_2$ or direct electron doping in $Ca_{0.85}La_{0.15}Co_{1.89}As_2$. The results reported herein demonstrate the general possibility of amplifying minor localized electronic effects to achieve major changes in material's properties via involvement of strongly correlated electrons.

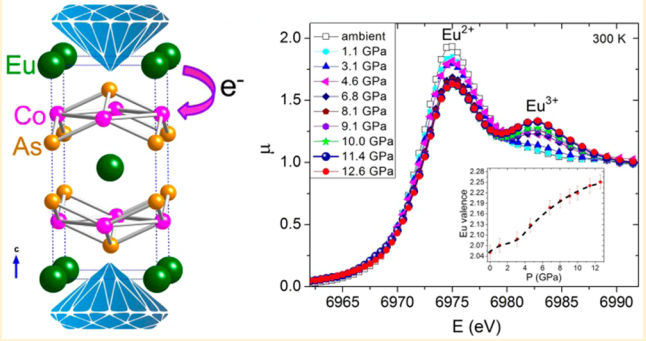

INTRODUCTION

Itinerant magnets represent a peculiar class of materials that exhibit strong correlations between their electronic structure and magnetic properties. As a result, the magnetic behavior of itinerant systems can be very sensitive to electronic doping caused by chemical substitution, applied pressure, or magnetic field, even if such perturbations are small. In particular, as relevant to the present work, minor perturbations in $ThCr_2Si_2$-type intermetallics have been shown to induce superconductivity,[1] quantum phase transitions,[2] metal−insulator transitions,[3] ferromagnetic semiconductivity,[4] and so on. Surprisingly, however, the potential to use chemical changes to modify and control the properties of itinerant magnets remains underexplored, despite the increasing interest to their chemically sensitive magnetic behavior, which offers a rich chemistry playground.[5]

One of the most fascinating changes in the magnetic properties of itinerant systems was reported by Jeitschko and co-workers for $EuCo_2P_2$. This material exhibits a pressure-induced first-order phase transition that involves a structural collapse associated with the valence change of Eu from +2 to +3 and a simultaneous change in the magnetic behavior.[6,7] The ambient, low-pressure (LP) form of $EuCo_2P_2$ contains Eu^{2+} ions and shows antiferromagnetic (AFM) ordering of 4f moments at T_N^{Eu} = 66 K, whereas Co moments are not involved in the magnetic ordering. Above 3.1 GPa, however, the change in the Eu oxidation state from +2 to +3 leads to the emergence of itinerant 3d magnetism in the Co sublattice of the high-pressure (HP) form, which orders AFM at T_N^{Co} = 260 K.

Received: December 3, 2015
Published: February 3, 2016

ACS Publications © 2016 American Chemical Society

DOI: 10.1021/jacs.5b12659
J. Am. Chem. Soc. 2016, 138, 2724−2731

Table 1. Data Collection and Structure Refinement Parameters for $Ca_{0.9}Eu_{0.1}Co_{1.91}As_2$ and $Ca_{0.85}La_{0.15}Co_{1.89}As_2$[a]

nominal composition	$EuCo_2As_2$	$CaCo_2As_2$	$Ca_{0.9}Eu_{0.1}Co_2As_2$	$Ca_{0.9}La_{0.1}Co_2As_2$
refined formula	$EuCo_2As_2$	$CaCo_{1.87(1)}As_2$	$Ca_{0.901(3)}Eu_{0.099(3)}Co_{1.906(8)}As_2$	$Ca_{0.845(4)}La_{0.155(4)}Co_{1.88(1)}As_2$
Ca/R (EDX analysis)			0.88(1): 0.12(1)	0.84(2): 0.16(2)
temperature, K	293	293	293	293
λ (Å)	0.71073	0.71073	0.71073	0.71073
space group	*I*4/*mmm*	*I*4/*mmm*	*I*4/*mmm*	*I*4/*mmm*
unit cell *a* (Å)	3.929(1)	3.9927(2)	3.9984(2)	4.0018(2)
c (Å)	11.512(4)	10.3133(6)	10.3696(2)	10.3726(8)
V (Å^3)	177.8(1)	164.42(1)	165.79(9)	166.11(2)
Z	2	2	2	2
crystal size (mm^3)	0.05 × 0.05 × 0.02	0.03 × 0.02 × 0.02	0.06 × 0.04 × 0.01	0.06 × 0.03 × 0.02
ρ_{calc} (g cm^{-3})	7.843	6.217	6.390	6.351
μ (mm^{-1})	44.861	31.324	32.767	32.100
θ_{max} (deg)	36.295	42.02	44.929	45.316
reflections collected	1302	1464	1823	1292
unique reflections	160	206	235	232
parameters refined	10	10	11	10
R_{int}	0.019	0.020	0.026	0.034
R_1, wR_2 [$F_0 > 4\sigma(F_0)$]	0.019, 0.049	0.020, 0.048	0.026, 0.058	0.026, 0.064
diff. peak and hole (e Å^{-3})	1.31, −2.72	1.41, −1.28	0.93, −2.23	1.81, −1.50
goodness-of-fit	1.26	1.16	1.20	1.19

[a]The crystal structure refinements of $EuCo_2As_2$ and $CaCo_2As_2$ are shown for comparison. Further details of the crystal structure determination of $Ca_{0.9}Eu_{0.1}Co_{1.91}As_2$ and $Ca_{0.85}La_{0.15}Co_{1.89}As_2$ may be obtained from Fachinformationszentrum Karlsruhe, D-76344 Germany, on quoting the depository numbers CSD-430337 and CSD-430338, respectively.

A related isostructural compound $EuCo_2As_2$ also exhibits AFM ordering of Eu^{2+} 4f moments at $T_N^{Eu} \approx 40$ K at ambient pressure.[8,9] A recent report revealed a second-order structural collapse in this material.[10] Although pressure-induced changes to magnetic properties were not reported, we hypothesized that $EuCo_2As_2$ might also exhibit pressure-induced valence change toward Eu^{3+}, which would lead to itinerant magnetism. Moreover, we might expect the ordering to be ferromagnetic (FM), given our recent report of ferromagnetism in LP-RCo_2As_2 (R = La, Ce, Pr, and Nd) that contain R^{3+} ions.[11]

Herein we report a remarkable emergence of itinerant 3d ferromagnetism in $EuCo_2As_2$ under the unifying effect of physical pressure, chemical compression, and aliovalent (non-isoelectronic) substitution. The pressure-induced FM ordering in $EuCo_2As_2$ is conclusively shown by X-ray absorption near-edge structure (XANES) and X-ray magnetic circular dichroism (XMCD) spectroscopy and supported by the band structure calculations. In striking contrast to HP-$EuCo_2P_2$, which contains mainly Eu^{3+} ions, HP-$EuCo_2As_2$ exhibits the stabilization of a mixed-valent $Eu^{2.25+}$ state that persists even in the collapsed structure up to 12.6 GPa, the maximum pressure achieved in our experiments. Furthermore, we demonstrate the generality of this phenomenon in the present system by inducing valence changes via chemical compression in $Ca_{0.9}Eu_{0.1}Co_{1.91}As_2$ and via direct electron doping in $Ca_{0.85}La_{0.15}Co_{1.89}As_2$. In all instances, the mixed valence achieved in the electropositive metal site perturbs the electronic band structure and 3d band population, causing FM ordering of Co moments.

MATERIALS AND METHODS

Starting Materials. Finely dispersed powders of arsenic (99.99%) and lanthanum (99.9%), calcium dendritic pieces (99.98%), and bismuth granules (99.997%) were obtained from Alfa Aesar. Eu metal chunks (>99%) were acquired through the Materials Preparation Center at Ames Laboratory, which is supported by the U.S. Department of Energy, Basic Energy Sciences. Eu and Ca metals were cut into small pieces. Cobalt powder (Alfa Aesar, 99.5%) was additionally purified by heating under a flow of H_2 gas at 773 K for 5 h. All manipulations during sample preparation were carried out in an argon-filled drybox (content of O_2 < 1 ppm).

Caution! *Arsenic is a toxic element and should be handled and disposed of following proper safety procedures. It is recommended to use a protective mask when preparing or grinding As-containing samples.*

Synthesis. The starting materials for the synthesis of $EuCo_2As_2$ were mixed in the Eu/Co/As/Bi = 2:2:2:30 ratio (total mass = 5 g) and loaded into 10 mm inner diameter (i.d.) carbonated silica tubes, which were then sealed under vacuum (<10^{-2} mbar). An excess amount of Eu metal was required for the preparation of phase-pure product. The mixtures were annealed at 1223 K for 8 days and cooled down by turning off the furnace. The Bi flux was removed by soaking the sample in a mixture of glacial acetic acid and 30% aqueous H_2O_2 (1:1 v/v) for 4−6 days, followed by washings with dilute HCl (1:1 v/v) and water. The phase purity of obtained products was checked by powder X-ray diffraction. X-ray quality platelike single crystals with size up to ∼1 × 1 × 0.1 mm^3 were also obtained during the reaction. Larger crystals (∼2 × 2 × 0.2 mm^3) for single-crystal neutron diffraction experiments were prepared by scaling up the total mass of reactants to 25 g (of which 23.5 g was Bi flux) and using larger carbonated silica tubes with a 15 mm i.d. The synthesis of $CaCo_{1.87}As_2$, $Ca_{0.9}Eu_{0.1}Co_{1.91}As_2$, and $Ca_{0.85}La_{0.15}Co_{1.89}As_2$ was performed using analogous procedures.

Single-Crystal X-ray Diffraction. In a typical experiment, a single crystal was glued on the tip of a quartz fiber and mounted on a goniometer head of a Bruker AXS SMART diffractometer with an APEX-II CCD detector. Data were collected at 293 K with ω scans in steps of 0.3° and integrated with the Bruker SAINT software.[12] Crystal structures were solved and refined with the SHELX suite of program in the *I*4/*mmm* space group (No. 139).[13] During the refinement of $Ca_{0.9}R_{0.1}Co_2As_2$ (R′ = Eu and La) structures, the Ca and R positions were constrained to have equal atomic displacement parameters. A summary of pertinent information relating to unit cell parameters, data collection, and refinements is provided in Table 1.

Physical Measurements. Elemental analysis of selected single crystals was carried out on a JEOL 5900 scanning electron microscope with an energy-disperse X-ray (EDX) microanalysis. Magnetic measurements were performed on an oriented single crystal or

DOI: 10.1021/jacs.5b12659
J. Am. Chem. Soc. 2016, 138, 2724−2731

polycrystalline powders with a Quantum Design SQUID magnetometer MPMS-XL; dc magnetization was measured in an applied field of 1 mT, 0.1 T, or 0.2 T in the 1.8−300 K range. Field-dependent magnetization was measured at 1.8 K with the applied magnetic field varying from 0 to 7 T.

Neutron Diffraction. Single-crystal and powder neutron diffraction experiments were performed at the High-Flux Isotope Reactor at Oak Ridge National Laboratory. A large single crystal of $EuCo_2As_2$ (~2 × 2 × 0.2 mm^3) was mounted on the stage of the HB-3A four-circle single-crystal diffractometer. Neutrons with wavelength of λ = 1.003 Å were generated from bent silicon monochromator.[14] The data were collected at 60 and 5 K. The selected (0 0 2.79) magnetic peak was measured as a function of temperature to determine the magnetic ordering temperature. Absorption correction was applied using the PLATON software.[15] The nuclear and magnetic structure refinements were performed with the FULLPROF software.[16] Powder neutron diffraction experiments on $CaCo_{1.87}As_2$ were carried out using the HB-2A high-resolution neutron powder diffractometer. The sample was held in a cylindrical vanadium container placed in a top-loading closed-cycle refrigerator. The data were collected at 1.5 K with the wavelength λ = 2.406 Å. Rietveld refinement was carried out using FULLPROF.[16]

X-ray Absorption Near-Edge Structure and X-ray Magnetic Circular Dichroism Measurements. High-pressure XANES and XMCD spectra of $EuCo_2As_2$ and $EuCo_2P_2$ were measured at the Eu L_3 edge using a transmission geometry at beamline 4-ID-D of the Advanced Photon Source, Argonne National Laboratory. A membrane-driven CuBe diamond anvil cell (DAC) was prepared with a partially perforated anvil placed opposite to a fully perforated anvil with a mini anvil on top. The culet diameter was 600 μm. A 250 μm hole was drilled as sample chamber on a stainless-steel gasket preindented to a thickness of 80 μm. A polycrystalline sample of $EuCo_2As_2$ or $EuCo_2P_2$ was ground and sieved though a mesh to afford a fine powder with grain size of ~4−5 μm, which was then mixed with silicon oil used as pressure-transmitting medium. A few ruby chips were also loaded with the sample for pressure calibration. The DAC was inserted into a 6.5 T magnet equipped with a helium flow system for cooling down to 1.4 K. The pressure was controlled and calibrated in situ using the He gas membrane and an on-line ruby luminescence system inserted into one of the radial re-entrant bores of the split superconducting magnet. The XMCD experiments were performed with magnetic field applied parallel and antiparallel to the incident photon wave vector to remove any artifact signal. XANES spectra of $Ca_{0.9}Eu_{0.1}Co_{1.91}As_2$ were obtained at the Eu L_3 edge in a transmission mode using Si(111) monochromator. The experiment was performed at the beamline mySpot of BESSY-II storage ring (HZB, Berlin, Germany).

Quantum−Chemical Calculations. Density functional band structure calculations and the interatomic crystal orbital Hamilton population (COHP) analysis were performed with the tight-binding−linear-muffin-tin-orbitals−atomic-sphere-approximation (TB-LMTO-ASA) software package.[17] The von Barth−Hedin exchange-correlation potential was applied for the local density approximation (LDA) calculation.[18] The radial scalar−relativistic Dirac equation was solved to obtain the partial waves. No empty spheres had to be added. The calculations contained a basis set of Eu 6s/5d/(6p) with Eu 4f treated as the core, Co 4s/4p/3d, and As 4s/4p/(4d) (downfolded orbitals in parentheses). The integrations were performed over the reciprocal unit cells based on a 12 × 12 × 24 mesh of 3456 *k*-points in the irreducible wedge of the Brillouin zone. The unit cell parameters were taken from the structural data at ambient pressure and 7.5 GPa as reported earlier.[10]

RESULTS AND DISCUSSION

Synthesis and Crystal Structures. As shown in our previous work, reactions in Bi flux provide an effective method for the preparation of phase-pure ternary arsenides and the growth of representative single crystals.[11,19] Using this approach, the polycrystalline and single-crystal samples of $EuCo_2As_2$, $Ca_{0.9}Eu_{0.1}Co_{1.91}As_2$, and $Ca_{0.85}La_{0.15}Co_{1.89}As_2$ were obtained by annealing a mixture of elements in Bi flux at 1223 K. The flux was subsequently removed by washing with a mixture of H_2O_2 and glacial CH_3COOH. For the purpose of comparing the structures of $Ca_{0.9}Eu_{0.1}Co_{1.91}As_2$ and $Ca_{0.85}La_{0.15}Co_{1.89}As_2$ with that of the parent compound, we also prepared $CaCo_{1.87}As_2$ in the similar fashion. The phase purity of products obtained was confirmed by powder X-ray diffraction.

On the basis of single-crystal X-ray diffraction data, the crystal structures were solved in the *I*4/*mmm* space group, with all compounds being of the $ThCr_2Si_2$ structure type (Table 1). The refinement of the single-crystal compositions led to the Ca/Eu and Ca/La ratios that were in good agreement with the results of EDX analysis and also close to those of the nominal compositions (Table 1). The crystal structure refinements also revealed vacancies in the Co sites for all but the $EuCo_2As_2$ structure. The presence of vacancies in $CaCo_2As_2$ was also confirmed by the Rietveld refinement of neutron powder diffraction data that resulted in the composition $CaCo_{1.89}As_2$ (Figure S1 and Table S1). These findings are in agreement with the observation of Co vacancies both in $CaCo_{1.86}As_2$ obtained via Sn-flux method[20,21] and in $RCo_{2-\delta}As_2$ (R = La−Nd) prepared in Bi flux or by solid-state reactions.[11,19,22] The full occupancy of the Co site in the crystal structure of $EuCo_2As_2$ also agrees with the previous report.[8]

The structures are built of $[Co_2As_2]$ layers that alternate along the *c* axis with layers of electropositive atoms (Figure 1).

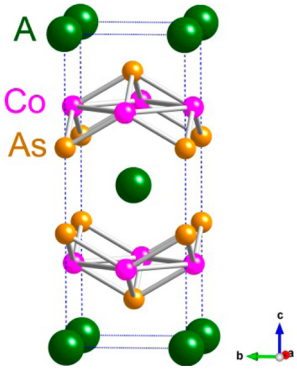

Figure 1. Crystal structure of ACo_2As_2 (A = Ca and Eu). Color scheme: A = green, Co = magenta, and As = yellow.

In all structures, the $[Co_2As_2]$ layer is held together by Co−As bonds at ~2.34 Å (Table 2). The Co−Co intralayer distance, which is related to the unit cell parameter, $d_{Co-Co} = a/\sqrt{2}$, equals 2.8233(1) Å in $CaCo_{1.87}As_2$ and 2.7782(9) Å in $EuCo_2As_2$. Because the ionic radius of Eu^{2+}(1.25 Å) is substantially larger than that of Ca^{2+} (1.12 Å), the As−As distance, which defines the separation between the $[Co_2As_2]$ layers along the *c* axis, changes dramatically from 2.73 Å in

Table 2. Interatomic Distances in the Crystal Structures of $EuCo_2As_2$, $CaCo_{1.87}As_2$, $Ca_{0.9}Eu_{0.1}Co_{1.91}As_2$, and $Ca_{0.85}La_{0.15}Co_{1.89}As_2$

compound	Co−Co (Å)	Co−As (Å)	As−As (Å)
$EuCo_2As_2$	2.7782(9)	2.3441(7)	3.198(2)
$CaCo_{1.87}As_2$	2.8233(1)	2.3351(2)	2.7342(9)
$Ca_{0.9}Eu_{0.1}Co_{1.91}As_2$	2.8274(1)	2.3390(2)	2.7563(8)
$Ca_{0.85}La_{0.15}Co_{1.89}As_2$	2.8297(1)	2.3372(4)	2.771(1)

DOI: 10.1021/jacs.5b12659
J. Am. Chem. Soc. 2016, 138, 2724−2731

$CaCo_{1.87}As_2$ to 3.20 Å in $EuCo_2As_2$. In the structures of $Ca_{0.9}Eu_{0.1}Co_{1.91}As_2$ and $Ca_{0.85}La_{0.15}Co_{1.89}As_2$, both the Co−Co and As−As distances increase slightly compared to those of $CaCo_{1.87}As_2$, confirming the successful substitution of Eu or La for Ca atoms.

LP-$EuCo_2As_2$: Magnetic Structure. A large platelike crystal ($2 \times 2 \times 0.2$ mm^3) was used for magnetic susceptibility and neutron diffraction studies on $EuCo_2As_2$ at ambient pressure. The temperature dependence of magnetic susceptibility (χ) confirms the AFM ordering of Eu^{2+} 4f moments in the *ab* plane at T_N = 47 K (Figure 2a), which agrees with the

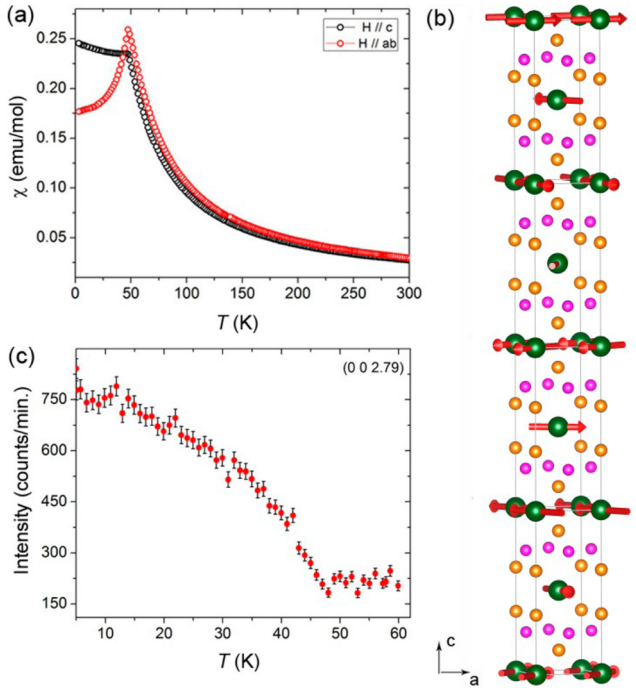

Figure 2. (a) Temperature dependence of field-cooled magnetic susceptibility measured on an oriented single crystal of $EuCo_2As_2$ in the applied magnetic field of 0.1 T. (b) Magnetic structure of $EuCo_2As_2$ (Eu = green, Co = magenta, and As = yellow). (c) Integrated intensity of the (0 0 2.79) magnetic peak as a function of temperature.

previous reports.[8,9] Fitting the high-temperature dependence of $^1/_\chi$ to the Curie−Weiss law resulted in a positive Weiss constant of θ = 20 K, which indicates FM nearest-neighbor interactions.

The magnetic structure of $EuCo_2As_2$ was established by single-crystal neutron diffraction. The magnetic structure refinement showed the presence of ordered magnetic moments only on Eu sites. (The moment refined on the Co site was zero within an esd of 0.2 μ_B.) The 4f moments align FM in the *ab* plane of the tetragonal lattice, but adopt an incommensurate AFM spiral structure with a propagation *k*-vector of (0, 0, 0.79) along the *c* axis (Figure 2b). The ordering temperature, determined from the dependence of integrated intensity of (0 0 2.79) magnetic peak (Figure 2c), coincided with the value of 47 K obtained from the susceptibility data. The refined moment for Eu was 7.26(8) μ_B, close to the theoretical expectation of 7.0 μB per Eu^{2+} ion. The magnetic ordering and magnetic structure of $EuCo_2As_2$ at ambient pressure are very similar to those of $EuCo_2P_2$, which also exhibits the AFM spiral structure with k = (0, 0, 0.85).[23]

$EuCo_2As_2$: XANES and XMCD Spectra. The previous X-ray powder diffraction study revealed that $EuCo_2As_2$ undergoes a structural collapse at 4.7 GPa,[10] although it is a second-order transition, not a first-order one as seen in $EuCo_2P_2$.[7] To study the effect of pressure on the magnetic behavior of $EuCo_2As_2$, we carried out Eu L_3 XANES and XMCD measurements on a polycrystalline sample that was ground and sieved to afford a fine powder with ∼4−5 μm particle size. At ambient pressure and 300 K, a single absorption peak was observed at 6.975 keV, corresponding to the Eu^{2+} state (Figure 3a). At 3.1 GPa, a weak

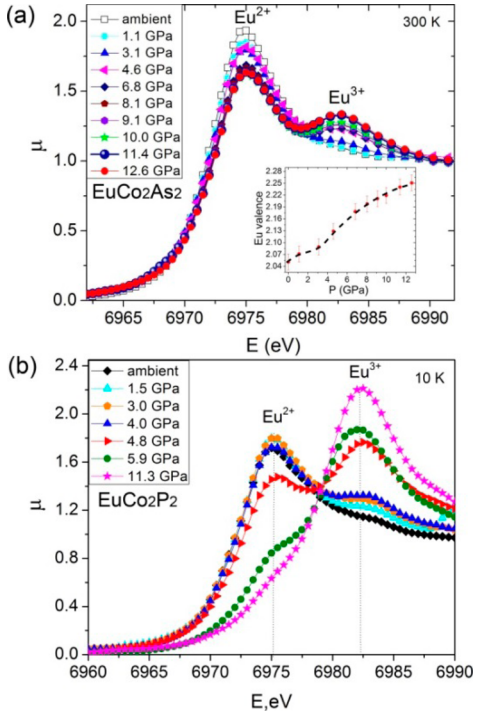

Figure 3. (a) Eu L_3 XANES spectra of $EuCo_2As_2$ at 300 K and variable pressure. Inset: the average Eu valence as a function of pressure. (b) Eu L_3 XANES spectra of $EuCo_2P_2$ at 10 K and variable pressure.

peak at 6.983 keV became resolved, indicating the evolution of the Eu^{3+} state. As the pressure increased, the intensity of the Eu^{3+} peak continued to grow, with a concomitant suppression of the Eu^{2+} contribution. The intensity redistribution slowed down at higher pressure, although the concentration of Eu^{3+} continued to increase even above 11.4 GPa. A similar behavior was observed at 4.2 K (Figure S2). These observations indicate the stabilization of a mixed-valent Eu state in $EuCo_2As_2$ under applied pressure. Such behavior differs drastically from that of $EuCo_2P_2$, which showed a nearly complete conversion from the Eu^{2+} to the Eu^{3+} state as the pressure was increased (Figure 3b).

The evaluation of the average Eu oxidation state from the XANES spectra revealed that the critical pressure for the second-order phase transition in $EuCo_2As_2$ is ∼4.6 GPa (valence inflection point in Figure 3a, inset) which agrees well with the value of 4.7 GPa established by powder X-ray diffraction.[10] The maximum oxidation state achieved at 12.6 GPa was +2.25(2). In contrast, $EuCo_2P_2$ exhibits a nearly pure Eu^{3+} state above 6 GPa (Figure 3b). The pressure-induced valence change in $EuCo_2As_2$ is reversible; the Eu^{2+} state was restored after the pressure had been released.

DOI: 10.1021/jacs.5b12659
J. Am. Chem. Soc. 2016, 138, 2724−2731

To probe the nature of magnetic ordering in the Eu sublattice, we recorded 4.2 K XMCD spectra at 1.0 and 7.5 GPa, i.e., below and above the critical pressure for the phase transition observed for $EuCo_2As_2$. XMCD at Eu L_3 absorption edge is sensitive to the ordering of 4f moments by means of intra-atomic 4f−5d exchange.[24] The XMCD signal thus provides a measure of magnetization in the 4f sublattice. A weak XMCD signal at 1 GPa (blue curve in Figure 4a) was

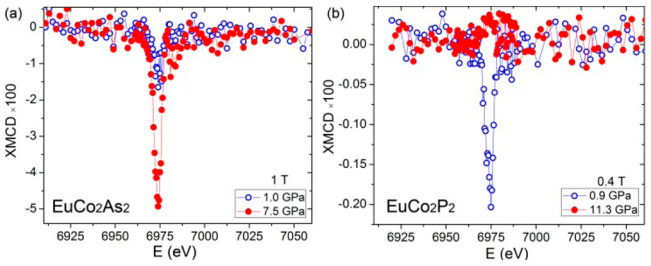

Figure 4. (a) Eu L_3 XMCD spectra of $EuCo_2As_2$ at 1.0 and 7.5 GPa measured at 4.2 K and 1 T. (b) Eu L_3 XMCD spectra of $EuCo_2P_2$ at 0.9 and 11.3 GPa measured at 10 K and 0.4 T.

attributed to a small FM component that appears when the AFM-ordered Eu^{2+} moments are canted by the 1 T applied magnetic field. A similar weak signal was also observed in the XMCD spectrum of $EuCo_2P_2$ at 0.9 GPa (Figure 4b; compare the scale to that in Figure 4a). When the pressure was increased to 11.3 GPa, the XMCD peak vanished for $EuCo_2P_2$, which is in agreement with the nearly complete transition to the nonmagnetic Eu^{3+} ground state. For $EuCo_2As_2$, however, the amplitude of the XMCD signal increased dramatically under 7.5 GPa (red curve). Keeping in mind that the partial (25%) $Eu^{2+}\rightarrow Eu^{3+}$ transition established from the XANES spectra should decrease the concentration of the magnetic Eu^{2+} centers, the drastic increase in the Eu L_3 XMCD signal in HP-$EuCo_2As_2$ suggests a change in the character of the magnetically ordered state.

Indeed, the field dependence of the XMCD signal amplitude of $EuCo_2As_2$ measured at 4.2 K and 7.5 GPa reveals magnetization behavior that is indicative of a FM or ferrimagnetic (FiM) rather than AFM ordering (Figure 5a).

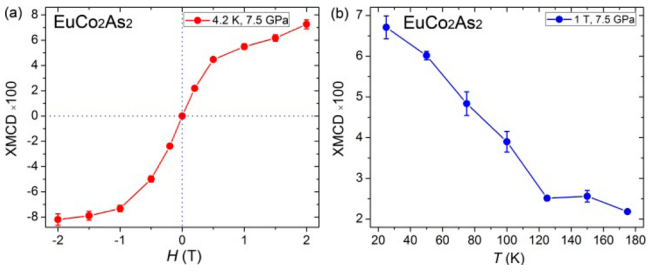

Figure 5. (a) Field and (b) temperature dependences of the 7.5 GPa Eu L_3 XMCD amplitude for $EuCo_2As_2$ measured at the temperature of 4.2 K and at the applied magnetic field of 1 T, respectively.

The temperature dependence of the XMCD signal amplitude as order parameter measured at 7.5 GPa and 1 T also suggests FM or FiM ordering with T_C = 125 K (Figure 5b). Moreover, this finding lends support to the pressure-induced itinerant magnetism in the Co sublattice, as will be discussed below.

It is possible that the strong XMCD at Eu L_3 edge in HP-$EuCo_2As_2$ also has a contribution from the ordering of Co 3d moments via the Eu(5d)−Co(3d) hybridization effect.[24] Unfortunately, we could not detect a measurable XMCD signal at the Co *K*-edge at 7.5 GPa, even when the field was increased to 2 T. On the one hand, the signal might be too weak, taking into account that the moment per Co atom in other RCo_2As_2 phases is ∼0.5 μ_B[11] and that the *K*-edge absorption probes the s → p transitions, thus involving the 3d electron density only indirectly. On the other hand, the use of softer X-rays to probe the Co $L_{2,3}$ edge is incompatible with the DAC used in the experiments under pressure.

In $EuCo_2P_2$, the transition from the localized Eu 4f magnetism in the LP phase to the itinerant Co 3d magnetism in the HP phase is accompanied by the dramatic increase in T_N from 66 to 260 K.[6] The magnetic behavior of HP-$EuCo_2P_2$ is reminiscent of that observed at ambient pressure for RCo_2P_2 materials (R = Ce, Pr, and Nd), which show AFM ordering of Co moments above 300 K. Likewise, the ordering temperature in HP-$EuCo_2As_2$ (T_C = 125 K) is much higher than the value of T_N = 47 K for LP-$EuCo_2As_2$. Moreover, the T_C falls in the range established for the FM ordering of Co moments in RCo_2As_2 materials, $T_C \approx$ 60−200 K.[11] Hence, we believe that these findings support the emergence of FM ordering in the Co sublattice of HP-$EuCo_2As_2$.

$EuCo_2As_2$: Electronic Structure. To obtain additional support for the possibility of the pressure-induced FM ordering of Co 3d moments in HP-$EuCo_2As_2$, we performed electronic band structure calculations using the structural parameters determined for $EuCo_2As_2$ at ambient pressure and at 7.5 GPa.[10] A comparison of the density of states (DOS) at different pressures reveals a substantially stronger contribution from the Co 3d orbitals at the Fermi level (E_F) in the HP structure (Figure 6a). The product of the exchange constant (J_{Co-Co})[25] and the Co 3d DOS at E_F (N_F) increased from 0.67 at ambient pressure to 1.07 at 7.5 GPa. Thus, the Stoner criterion for ferromagnetism (JN_F > 1) becomes satisfied only in the HP-$EuCo_2As_2$.

It is interesting to point out that the applied pressure alters both the character of the 3d DOS in the vicinity of the Fermi level and the filling of the 3d states due to the pressure-induced Eu(4f) → Co(3d) electron transfer. The latter becomes obvious from the changes observed in the COHP (Figure 6b). Although in the LP-$EuCo_2As_2$ structure the Fermi level crosses essentially nonbonding Co−Co states (COHP ≈ 0), in the HP-$EuCo_2As_2$ structure it crosses strongly antibonding states (−COHP < 0). Strong antibonding interactions in itinerant systems have been shown to promote magnetic ordering.[26] All these findings lend support to the hypotheses of itinerant Co 3d ferromagnetism in HP-$EuCo_2As_2$.

One can also consider a simplified picture of formal charges on the Co and As atoms during the pressure-induced structural collapse. In the LP-$EuCo_2As_2$, the large separation between the As atoms along the *c* axis suggests they have the formal −3 oxidation state. This results in the formal oxidation state of +2 for Co. In the collapsed structure of HP-$EuCo_2As_2$, the formation of a weakly covalent As−As interaction implies that the formal oxidation state of As becomes less negative whereas the oxidation state of Eu increases to +2.25 at 12.6 GPa. Both these factors should contribute to the decrease in the formal oxidation state of Co, or in other words, in the increased valence electron count per Co atom. This change agrees with the increase in the population of the Co−Co antibonding states under higher pressure as found by the band structure

DOI: 10.1021/jacs.5b12659
J. Am. Chem. Soc. 2016, 138, 2724−2731

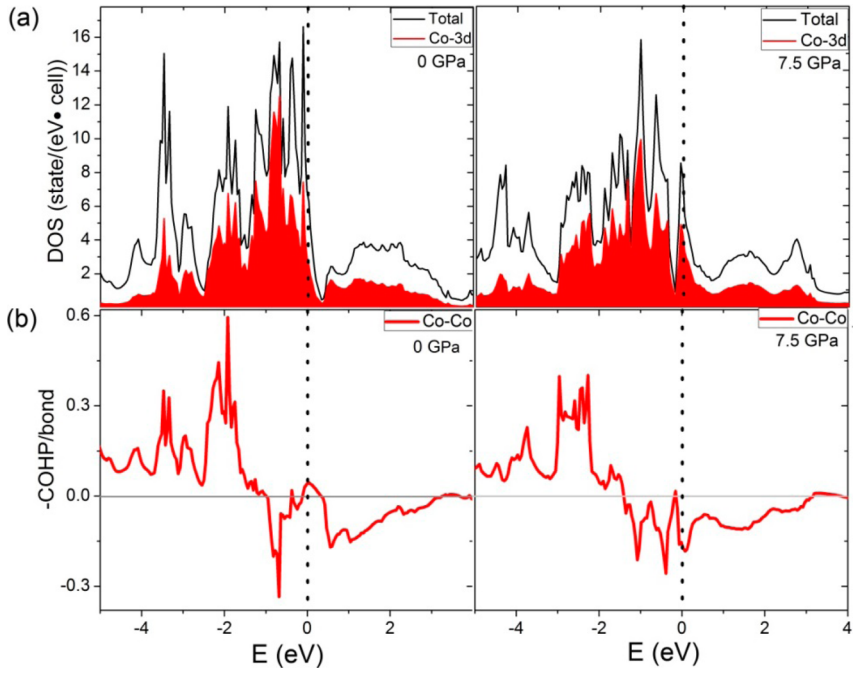

Figure 6. (a) Density of states and (b) Co−Co crystal orbital Hamilton population of $EuCo_2As_2$ at 0 GPa (left) and 7.5 GPa (right). The contribution from the Co 3d orbitals is shaded red. The Fermi level is indicated with a dotted black line.

calculations (Figure 6b). Furthermore, it is in line with similar observations made for $EuCo_2P_2$.[6,27]

$Ca_{0.9}Eu_{0.1}Co_{1.91}As_2$. To demonstrate further the effect of mixed valence on itinerant magnetism in this family of structures, we used chemical compression and direct electron doping to induce mixed valence in the electropositive crystallographic site of $CaCo_{1.87}As_2$ and increase the population of the Co 3d subband. Magnetic measurements on $CaCo_{1.87}As_2$ revealed AFM ordering at $T_N \approx 79$ K under ambient pressure (Figure S3), which is consistent with the behavior reported earlier.[28,29] The ionic radius of Ca^{2+} (1.12 Å) is closer to the ionic radius of Eu^{3+} (1.07 Å) than to the one of Eu^{2+} (1.25 Å). We have shown previously that such discrepancy in ionic radii can be used to induce a substantial chemical pressure on the Eu^{2+} site substituted into a lattice that is more appropriate to host Eu^{3+} ions.[30] To this end, we synthesized $Ca_{0.9}Eu_{0.1}Co_{1.91}As_2$ and examined it with XANES spectroscopy. The experiment revealed the average Eu oxidation state of +2.18 (Figure 7), confirming the successful achievement of the mixed-valent state by chemical compression.

The compound shows FM ordering with $T_C = 110$ K (Figure 8a). Given the low concentration of Eu sites, such ordering

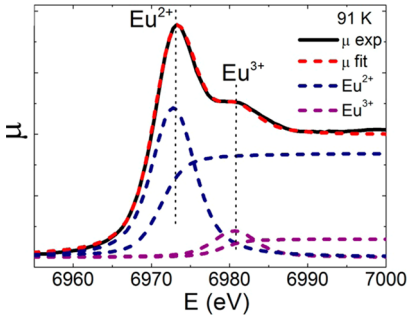

Figure 7. L_3 Eu XANES spectrum of $Ca_{0.9}Eu_{0.1}Co_{1.91}As_2$ at 91 K.

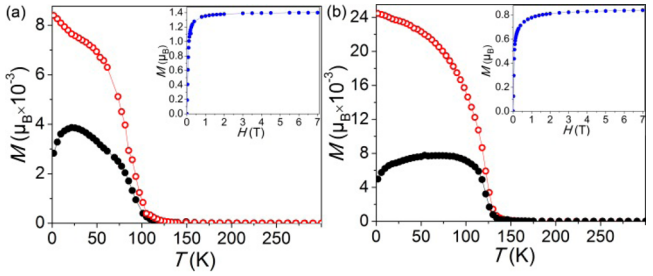

Figure 8. Temperature dependence of field-cooled (FC, red) and zero-field-cooled (ZFC, black) magnetization at 1 mT and field dependence of magnetization at 1.8 K (inset) for (a) $Ca_{0.9}Eu_{0.1}Co_{1.91}As_2$ and (b) $Ca_{0.85}La_{0.15}Co_{1.89}As_2$.

must originate, in the first place, from the Co sublattice. The theoretically expected moment from $Eu^{2.18+}$ state is 0.6 μ_B per $Ca_{0.9}Eu_{0.1}Co_{1.91}As_2$ formula unit (f.u.). Hence, the saturation magnetization of 1.4 μ_B at 1.8 K suggests FM coupling between Eu and Co moments, with the moment of 0.4 μ_B per Co atom. This value is similar to those observed for FM-ordered Co moments in RCo_2As_2.[11] The emergence of ferromagnetism in $Ca_{0.9}Eu_{0.1}Co_{1.91}As_2$ under ambient pressure is remarkable, given the AFM ordering in both $CaCo_{1.87}As_2$ and $EuCo_2As_2$ under the same conditions and especially the fact that only 0.018 of an electron per f.u. is transferred from the Eu 4f states to the Co 3d subband due to the chemical compression. This finding also indirectly supports the possibility of FM ordering of Co moments in the HP-$EuCo_2As_2$ that contains mixed-valent Eu sites.

$Ca_{0.85}La_{0.15}Co_{1.89}As_2$. To eliminate completely the influence of the Eu^{2+} magnetic moments and visualize the role of pure electron doping on the magnetic behavior of Co sublattice, we substituted 10% of Ca^{2+} ions in $CaCo_{1.87}As_2$ with diamagnetic La^{3+} (ionic radius 1.16 Å). The formula $Ca_{0.85}La_{0.15}Co_{1.89}As_2$, established by the X-ray crystal structure determination and EDX analysis, suggests that 0.15 extra

DOI: 10.1021/jacs.5b12659
J. Am. Chem. Soc. 2016, 138, 2724−2731

electrons per f.u. are donated into the Co 3d subband upon the partial substitution of La^{3+} for Ca^{2+} ions. $Ca_{0.85}La_{0.15}Co_{1.89}As_2$ exhibits FM ordering at T_C = 130 K, with the saturation magnetization of 0.4 μ_B per Co atom (Figure 8b). Both values are in excellent agreement with those observed for $Ca_{0.9}Eu_{0.1}Co_{1.91}As_2$, thus confirming that it is indeed the electron doping into the Co layer that induces itinerant ferromagnetism in HP-$EuCo_2As_2$, $Ca_{0.9}Eu_{0.1}Co_{1.91}As_2$, and $Ca_{0.85}La_{0.15}Co_{1.89}As_2$.

The extent of electron transfer required to trigger the FM ordering of Co moments in $Ca_{0.9}Eu_{0.1}Co_{1.91}As_2$ (0.018 electrons per f.u.) is much smaller than the electron transfer achieved in $Ca_{0.85}La_{0.15}Co_{1.89}As_2$ (0.15 electrons per f.u.). Thus, the FM ordering in $Ca_{1-x}La_xCo_{2-y}As_2$ can be expected even at lower doping levels of La.

It is also interesting to point out that the Co−Co distances increase slightly upon substitution of Eu or La for Ca in $CaCo_{1.87}As_2$ (see Table 2). Such increase appears normal for $Ca_{0.85}La_{0.15}Co_{1.91}As_2$ because the Co−Co distance in $LaCo_2As_2$ (2.8634 Å)[11] is larger than the one in $CaCo_{1.87}As_2$ (2.8233 Å). In contrast, the Co−Co distance in $EuCo_2As_2$ (2.7782 Å) is substantially smaller than the one in $CaCo_{1.87}As_2$. The increase in the interlayer Co−Co separation in $Ca_{0.9}Eu_{0.1}Co_{1.91}As_2$ might be related to the emergence of FM ordering in the Co sublattice. Indeed, our previous studies of isostructural solid solutions $La_{1-x}R_xCo_2P_2$ (R = Pr and Nd) demonstrated that the FM ordering always favors longer Co−Co distances.[31,32]

These observations call for a more detailed investigation of the nonlinear change in the *a* parameter and Co−Co distances and the extent of doping required to trigger ferromagnetism in the Co sublattice. These questions can be addressed by studying the entire range of solid solutions $Ca_{1-x}Eu_xCo_{2-y}As_2$ and $Ca_{1-x}La_xCo_{2-y}As_2$. The work on these systems is currently under way in our laboratories, and the results will be reported in due course.

CONCLUSIONS

We have investigated the valence changes and magnetic phase transitions in ACo_2As_2 (A = Eu and Ca) as influenced by physical pressure, chemical compression, and aliovalent substitution. All these factors induce mixed valence in the electropositive metal A-site, causing electron doping into the Co 3d subband. The pressure-induced structural phase transition in $EuCo_2As_2$ around 4.7 GPa induces mixed valence with the average oxidation state of Eu equal to +2.25. This change in the electronic structure breaks down the AFM ordering in the Eu sublattice because both Eu (4f) and Co (3d) moments become FM-ordered with T_C = 125 K in HP-$EuCo_2As_2$. Although the FM ordering of Eu 4f moments was confirmed directly by XMCD experiment, the FM ordering of Co 3d moments was established indirectly by electronic band structure calculations and by investigation of $Ca_{0.9}Eu_{0.1}Co_{1.91}As_2$ and $Ca_{0.85}La_{0.15}Co_{1.89}As_2$. In the latter compounds, the itinerant 3d ferromagnetism in the Co sublattice is triggered by mixed valence of the A site due to chemical compression and by direct electronic doping into the Co layer due to aliovalent substitution, respectively.

This work demonstrates the highly sensitive nature of itinerant magnetism in $EuCo_2As_2$ and $CaCo_2As_2$ to electronic doping effects and the unifying action of physical pressure, chemical compression, and aliovalent substitution on triggering the electronic doping to achieve dramatic changes in the magnetism of these systems.

ASSOCIATED CONTENT

Supporting Information

The Supporting Information is available free of charge on the ACS Publications website at DOI: 10.1021/jacs.5b12659.

XANES spectra of $EuCo_2As_2$ at 4 K and DOS and COHP of $EuCo_2As_2$. (PDF)
Crystallographic information file for $EuCo_2As_2$. (CIF)
Crystallographic information file for $CaCo_{1.87}As_2$. (CIF)
Crystallographic information file for $Ca_{0.90}Eu_{0.10}Co_{1.91}As_2$. (CIF)
Crystallographic information file for $Ca_{0.845}La_{0.15}Co_{1.89}As_2$. (CIF)

AUTHOR INFORMATION

Corresponding Author

*E-mail: shatruk@chem.fsu.edu.

Present Addresses

C.M.T.: Department of Chemistry, Purdue University, 560 Oval Dr., West Lafayette, IN 47907, USA.
K.K.: Department of Chemistry, University of California, Davis, One Shields Ave., Davis, CA 95616, USA.

Funding

This work was supported by the National Science Foundation (Award DMR-1507233 to M.S.). The work at the Oak Ridge National Laboratory was sponsored by the Scientific User Facilities Division, Office of Basic Energy Sciences, U.S. Department of Energy (DOE). The use of the Advanced Photon Source at Argonne National Laboratory was supported by U.S. DOE under Contract No. DEAC02−06CH11357. A.P.M. and A.A.Y. thank the Russian Scientific Foundation (project 14−22−00098) for support.

Notes

The authors declare no competing financial interest.

ACKNOWLEDGMENTS

We acknowledge Helmholtz-Zentrum Berlin for providing the beamtime at the BESSY-II storage ring, Dr. Ivo Zizak and Dr. Dirk Wallacher for support during the experiment.

ABBREVIATIONS

HP, high-pressure; LP, low-pressure; FM, ferromagnetic; AFM, antiferromagnetic; FiM, ferromagnetic; XANES, X-ray absorption near-edge structure; XMCD, X-ray magnetic circular dichroism; DAC, diamond anvil cell; DOS, density of states; TB-LMTO-ASA, tight binding-linear muffin tin orbitals-atomic sphere approximation; LDA, local density approximation

REFERENCES

(1) (a) Rotter, M.; Pangerl, M.; Tegel, M.; Johrendt, D. *Angew. Chem., Int. Ed.* **2008**, *47*, 7949−7952. (b) Yuan, H. Q.; Singleton, J.; Balakirev, F. F.; Baily, S. A.; Chen, G. F.; Luo, J. L.; Wang, N. L. *Nature* **2009**, *457*, 565−568. (c) Torikachvili, M. S.; Bud'ko, S. L.; Ni, N.; Canfield, P. C. *Phys. Rev. Lett.* **2008**, *101*, 057006. (d) Han, J. T.; Zhou, J. S.; Cheng, J. G.; Goodenough, J. B. *J. Am. Chem. Soc.* **2010**, *132*, 908−909.

(2) Jia, S.; Jiramongkolchai, P.; Suchomel, M. R.; Toby, B. H.; Checkelsky, J. G.; Ong, N. P.; Cava, R. J. *Nat. Phys.* **2011**, *7*, 207−210.

(3) Mizoguchi, H.; Hosono, H. *J. Am. Chem. Soc.* **2011**, *133*, 2394−2397.

(4) Zhao, K.; Deng, Z.; Wang, X. C.; Han, W.; Zhu, J. L.; Li, X.; Liu, Q. Q.; Yu, R. C.; Goko, T.; Frandsen, B.; Liu, L.; Ning, F.; Uemura, Y. J.; Dabkowska, H.; Luke, G. M.; Luetkens, H.; Morenzoni, E.;

DOI: 10.1021/jacs.5b12659
J. Am. Chem. Soc. 2016, 138, 2724−2731

Dunsiger, S. R.; Senyshyn, A.; Böni, P.; Jin, C. Q. *Nat. Commun.* **2013**, *4*, 1442.
(5) Miller, G. J. *Chem. Soc. Rev.* **2006**, *35*, 799−813.
(6) Chefki, M.; Abd-Elmeguid, M. M.; Micklitz, H.; Huhnt, C.; Schlabitz, W.; Reehuis, M.; Jeitschko, W. *Phys. Rev. Lett.* **1998**, *80*, 802−805.
(7) Huhnt, C.; Schlabitz, W.; Wurth, A.; Mewis, A.; Reehuis, M. *Phys. Rev. B: Condens. Matter Mater. Phys.* **1997**, *56*, 13796−13804.
(8) Raffius, H.; Mörsen, E.; Mosel, B. D.; Müller-Warmuth, W.; Jeitschko, W.; Terbüchte, L.; Vomhof, T. *J. Phys. Chem. Solids* **1993**, *54*, 135−144.
(9) Ballinger, J.; Wenger, L. E.; Vohra, Y. K.; Sefat, A. S. *J. Appl. Phys.* **2012**, *111*, 07E106.
(10) Bishop, M.; Uhoya, W.; Tsoi, G.; Vohra, Y. K.; Sefat, A. S.; Sales, B. C. *J. Phys.: Condens. Matter* **2010**, *22*, 425701.
(11) Thompson, C. M.; Tan, X.; Kovnir, K.; Garlea, V. O.; Gippius, A. A.; Yaroslavtsev, A. A.; Menushenkov, A. P.; Chernikov, R. V.; Büttgen, N.; Krätschmer, W.; Zubavichus, Y. V.; Shatruk, M. *Chem. Mater.* **2014**, *26*, 3825−3837.
(12) *SMART and SAINT*; Bruker AXS Inc.: Madison, WI, 2007.
(13) Sheldrick, G. M. *Acta Crystallogr., Sect. A: Found. Crystallogr.* **2008**, *64*, 112−122.
(14) Chakoumakos, B. C.; Cao, H.; Ye, F.; Stoica, A. D.; Popovici, M.; Sundaram, M.; Zhou, W.; Hicks, J. S.; Lynn, G. W.; Riedel, R. A. *J. Appl. Crystallogr.* **2011**, *44*, 655−658.
(15) Spek, A. L. *Acta Crystallogr., Sect. D: Biol. Crystallogr.* **2009**, *65*, 148−155.
(16) Rodríguez-Carvajal, J. *Phys. B* **1993**, *192*, 55−69.
(17) Tank, R.; Jepsen, O.; Burkhardt, A.; Andersen, O. K. *The program TB-LMTO-ASA*, version 4.7; Max-Planck-Institut fur Festkorperforschung: Stuttgart, Germany, 1999.
(18) Von Barth, U.; Hedin, L. *J. Phys. C: Solid State Phys.* **1972**, *5*, 1629−1642.
(19) Thompson, C. M.; Kovnir, K.; Eveland, S.; Herring, M. J.; Shatruk, M. *Chem. Commun.* **2011**, *47*, 5563−5565.
(20) Quirinale, D. G.; Anand, V. K.; Kim, M. G.; Pandey, A.; Huq, A.; Stephens, P. W.; Heitmann, T. W.; Kreyssig, A.; McQueeney, R. J.; Johnston, D. C.; Goldman, A. I. *Phys. Rev. B* **2013**, *88*, 174420.
(21) Anand, V. K.; Dhaka, R. S.; Lee, Y.; Harmon, B. N.; Kaminski, A.; Johnston, D. C. *Phys. Rev. B: Condens. Matter Mater. Phys.* **2014**, *89*, 214409.
(22) Shen, S.; Wang, G.; Jin, S.; Huang, Q.; Ying, T.; Li, D.; Lai, X.; Zhou, T.; Zhang, H.; Lin, Z.; Wu, X.; Chen, X. *Chem. Mater.* **2014**, *26*, 6221−6225.
(23) Reehuis, M.; Jeitschko, W.; Möller, M. H.; Brown, P. J. *J. Phys. Chem. Solids* **1992**, *53*, 687−690.
(24) de Groot, F.; Kotani, A. *Core Level Spectroscopy of Solids*; CRC Press: Boca Raton, FL, 2008.
(25) The magnetic exchange constant for the intralayer Co−Co interactions can be approximated by the value established for the metallic cobalt in Janak, J. F. *Phys. Rev. B* **1977**, *16*, 255−262.
(26) Landrum, G. A.; Dronskowski, R. *Angew. Chem., Int. Ed.* **2000**, *39*, 1560−1585.
(27) Ni, B.; Abd-Elmeguid, M. M.; Micklitz, H.; Sanchez, J. P.; Vulliet, P.; Johrendt, D. *Phys. Rev. B* **2001**, *63*, 100102.
(28) Cheng, B.; Hu, B. F.; Yuan, R. H.; Dong, T.; Fang, A. F.; Chen, Z. G.; Xu, G.; Shi, Y. G.; Zheng, P.; Luo, J. L.; Wang, N. L. *Phys. Rev. B: Condens. Matter Mater. Phys.* **2012**, *85*, 144426.
(29) Ying, J. J.; Yan, Y. J.; Wang, A. F.; Xiang, Z. J.; Cheng, P.; Ye, G. J.; Chen, X. H. *Phys. Rev. B: Condens. Matter Mater. Phys.* **2012**, *85*, 214414.
(30) Kovnir, K.; Reiff, W. M.; Menushenkov, A. P.; Yaroslavtsev, A. A.; Chernikov, R. V.; Shatruk, M. *Chem. Mater.* **2011**, *23*, 3021−3024.
(31) Kovnir, K.; Thompson, C. M.; Zhou, H. D.; Wiebe, C. R.; Shatruk, M. *Chem. Mater.* **2010**, *22*, 1704−1713.
(32) Thompson, C. M.; Kovnir, K.; Garlea, V. O.; Choi, E. S.; Zhou, H. D.; Shatruk, M. *J. Mater. Chem. C* **2014**, *2*, 7561−7569.

DOI: 10.1021/jacs.5b12659
J. Am. Chem. Soc. 2016, 138, 2724−2731